Equilibrium geometries, electronic structure and magnetic properties of small manganese clusters

1998 J. Phys.: Condens. Matter 10 10863

(http://iopscience.iop.org/0953-8984/10/48/009)

J. Phys.: Condens. Matter **10** (1998) 10863–10877. Printed in the UK PII: S0953-8984(98)96099-4

Equilibrium geometries, electronic structure and magnetic properties of small manganese clusters

S K Nayak, B K Rao and P Jena

Physics Department, Virginia Commonwealth University, Richmond, VA 23284-20000, USA

Received 21 July 1998, in final form 25 August 1998

Abstract. The equilibrium geometries, electronic structure and magnetic properties of small Mn clusters consisting of up to five atoms have been calculated self-consistently using first principles molecular orbital theory. The electron–electron interaction has been accounted for using the local spin density and generalized gradient approximation to the density functional theory. The atomic orbitals forming the molecular orbital have been represented separately by Gaussian and numerical basis sets. Two different computer codes (Gaussian 94 and DMOL) were used to check the numerical consistency of our calculations. Mn_2 is found to be a weakly bound van der Waals molecule and its binding energy depends sensitively on the choice of basis set as well as the form of the exchange–correlation potential. The binding energies are less sensitive to these approximations in larger clusters. The binding improves with cluster size, but remains significantly lower than those in other transition metal clusters. The equilibrium geometries are fairly compact and symmetric although other isomers with distorted geometries and with nearly the same energy as that of the ground state do exist for Mn_5. The clusters also exhibit a variety of low-lying spin multiplicities, but the ground state spin configuration is ferromagnetic with a magnetic moment of 5 μ_B/atom. This not only contrasts with its bulk behaviour which is antiferromagnetic, but also differs from the behaviour in other transition-metal clusters where the magnetic moments/atom are always less than the free-atom value. The results are compared with available experiments on matrix isolated Mn clusters.

1. Introduction

Among all the elements in the first row of the transition metal series, manganese is unique as an atom, crystal or cluster. Its atomic configuration is $3d^5\ 4s^2$ and the promotion energy from $3d^5\ 4s^2$ to $3d^6\ 4s^1$ is very high, namely 2.14 eV [1]. This large promotion energy needed to alter the population of the outermost s and d shells reduces the degree of s–d hybridization as atoms are brought towards each other leading to weaker binding in clusters as well as in crystals. In the solid phase, it has many allotropic forms [2]. The stable form, known as α-Mn, is hard and brittle unlike other metals and has a very complex lattice structure with 54 atoms per unit cell. It has the lowest cohesive energy (2.92 eV), smallest bulk modulus (0.596×10^{11} N m^{-2}) and the highest compressibility of any of the elements in the 3d series. The properties of Mn clusters are also very different from other transition metal clusters. For example, Mn_2 is a weakly bonded van der Waals molecule with an estimated binding energy varying from 0.1 ± 0.1 eV to 0.56 ± 0.26 eV [3]. The bond length in rare-gas matrices is estimated to be 3.5 Å [4]. This is larger than the inter-atomic distances in the bulk which range from 2.25 Å to 2.95 Å. This is again in contrast to the normal behaviour of metal clusters (except those belonging to the alkaline-earth series, e.g. Mg) where the nearest neighbour distances increase with increasing cluster size [5].

0953-8984/98/4810863+15$19.50

Alkaline-earth atoms such as Mg have a filled s shell ($3s^2$), and Mg_2 is very weakly bound [6]. The transition from non-metallic to metallic bonding does not take place until the cluster contains about ten atoms [7]. Mn_2, however, poses additional challenges as its 3d orbital is half full whereas the inner orbital of Mg, $2p^6$ is completely full. This half-filled 3d orbital has interesting consequences for the magnetic properties of Mn_2 and larger clusters that do not arise in alkaline-earth clusters. To illustrate this, consider the molecular orbitals of Mn_2. As two Mn atoms are brought towards each other the 3d and 4s orbitals would split into bonding and antibonding states. If the coupling between the two atoms is weak, as it should be for a van der Waals system, the splitting of the d and s states should be small. The four s electrons will fill the bonding and the antibonding s states and will not contribute to the net magnetic moment. The ten d electrons, on the other hand, have a choice. They can all occupy the bonding orbital leading to zero total moment ($5\uparrow$ and $5\downarrow$ localized around the atomic sites). It is also possible that five electrons can occupy the bonding and the other five occupy the antibonding states. By lining up in the parallel direction, they can gain energy by exchange interaction. If this gain is larger than the energy difference between the bonding and antibonding states, the system will have a net moment of 10 μ_B. Thus, whether the ground state of Mn_2 is anti-ferromagnetic (0 μ_B) or ferromagnetic (10 μ_B) would depend on the two competing factors: the energy splitting and the exchange interaction. In the case of the Cr_2 dimer, which has the shortest bond of any 3d-dimer, this splitting is large and the total moment is zero. The coupling in the Cr_2 is known to be anti-ferromagnetic.

Experiments on Mn clusters in the beam have been very limited. This is because Mn_2 is a weakly bound molecule and to grow larger clusters, one needs to start from the dimer as a seed. Recently Parks *et al* [8] have succeeded in producing Mn clusters containing up to 70 atoms by cooling the inert gas condensation source to $-160\,^{\circ}$C. They studied the reaction of these clusters with H_2 and found that in small Mn_n clusters ($n \leqslant 15$), hydrogen atoms are unstable against H_2 desorption. They concluded [8] that this must arise due to the changing nature of bonding in these clusters. For small Mn_n clusters ($n \leqslant 15$), the bonding is perhaps weak, reminiscent of the van der Waals' bonding in Mn_2. The bonding becomes metallic for $n > 15$. Once the cluster is metallic, it is energetically possible to transfer charge from the metal cluster to the antibonding state of the H_2 molecule. The H–H bond consequently would break and H atoms would attach to the metal cluster atomically.

In a recent photoionization study of Mn clusters Koretsky and Knickelbein [9] have cast doubt on the nonmetal to metal transition in Mn_n clusters at $n = 15$. They have failed to observe any abrupt change in the ionization potential of these clusters in this size range which could signal the changing nature of the electronic structure. Thus, the origin of the changes in the reactivity of Mn clusters with hydrogen remains unresolved. Is it possible that the reactivity of hydrogen could be linked to the underlying magnetic structure of the clusters? While there are no magnetic measurements of Mn clusters in the beam, matrix isolation experiments [4] of Mn_3, Mn_4 and Mn_5 indicate that these clusters are ferromagnetically coupled with a magnetic moment of 5 μ_B/atom. Mn_2, on the other hand, was found to be antiferromagnetic as is the case with bulk Mn. Thus, Mn clusters at some critical size must undergo a transition from being ferromagnetic to antiferromagnetic. Could this occur at $n = 15$ and could this be linked to the onset of hydrogen reactivity?

Such questions are hard to answer as Mn clusters also pose a considerable challenge for theory. In addition to the traditional difficulties associated with the d electrons of the transition metals, the accounting for the weak bond between two Mn atoms requires very accurate calculations. Both the choice of basis functions and levels of correlation are expected to play major roles in the bonding in Mn clusters. Although there are a number of calculations on Mn_2 [10–15], the results concerning the binding energy, bond length

and spin multiplicity of Mn_2 conflict with each other. There are only two calculations on larger clusters. Shillady *et al* [14] studied the binding energy of Mn_5 using Hartree–Fock theory, but the geometry was confined to a pentagon. Fujima and Yamaguchi [15] have gone a step further and have examined the stability and chemical bonding in Mn_n clusters ($n \leqslant 7$) using the density functional theory and the local spin density approximation for a variety of geometries. The inter-atomic distances for each geometry were then optimized by minimizing the total energy. No attempts were made to carry out a global search for the equilibrium geometry nor did they attempt to find the preferred spin multiplicity by calculating total energies of all allowable spin configurations. For example, Mn_2 with 10 d electrons can have spin multiplicities of 1, 3, 5, 7, 9 and 11.

In this paper we present a comprehensive theoretical study of the equilibrium geometries, binding energies, electronic structure, ionization potential and magnetic properties of Mn_n clusters ($n \leqslant 5$) using different basis functions, levels of correlation and numerical procedures. For Mn_2, the calculations were carried out using the local spin density approximation (LSDA) and generalized gradient approximation (GGA) to the density functional theory. The atomic orbitals were represented using Gaussian as well as numerical basis sets. For the former, we used the Gaussian 94 software [16] while for the latter we used the DMOL code [17]. Calculations were repeated for spin multiplicities ranging from 1 to 11. For larger clusters, calculations were carried out using the Gaussian 94 code only. The geometries of Mn_3, Mn_4 and Mn_5 were obtained using a global optimization scheme at the GGA level of theory. We again searched for the preferred spin multiplicity by studying all possible values: 2 to 16 for Mn_3, 1 to 21 for Mn_4 and 2 to 26 for Mn_5. The bonding in Mn_2 is found to be weak and of the van der Waals type, but increases in larger clusters. The geometries are compact and symmetric with little Jahn–Teller distortion. The inter-atomic distances, in general, are larger than the bulk value. The most interesting results, however, concern the magnetic properties of the clusters. All clusters studied here, including Mn_2, are found to be ferromagnetic with a magnetic moment of 5 μ_B/atom.

In section 2 we present the details of our numerical computations. The results are compared with available theory and experiment in section 3. A summary of our conclusions is given in section 4.

2. Numerical procedure

Our calculations are based on the self-consistent field molecular orbital theory. Here the cluster wavefunction is a determinantal wavefunction formed out of molecular orbitals which are, in turn, constructed out of linear combination of atomic orbitals centred at the individual atomic sites. The coefficients of the linear combination are obtained self-consistently by solving the Raleigh–Ritz variational equation. The kinetic and electrostatic terms in the Hamiltonian are treated exactly while the exchange–correlation contribution is calculated using two approximations in the density functional theory. For the local spin density approximation (LSDA) we have used parameters determined by Vosko, Wilk and Nusair (VWN5) [18]. For the generalized gradient approximation (GGA) we have used the Becke form for exchange and the Perdew–Wang method for correlation (BPW91) [19] as well as the Becke hybrid form for exchange and the Lee–Yang–Parr form for correlation (B3LYP) [20]. To examine the role of basis sets in constructing the cluster orbitals, we have used three different basis functions in the Gaussian 94 software [16]. Basis 1 is an all-electron set (14s 9p 5d 1f/9s 5p 3d 1f) while basis 2 is an extended set obtained by augmenting basis 1 with diffuse functions (15s 11p 6d 1f/10s 7p 4d 1f). The third basis set (LANL2DZ) uses an effective core potential where 1s, 2s and 2p cores are frozen. For

Mn_2 we also repeated the calculations using the LSDA [18] and GGA [19] version of the density functional theory and the DMOL [17] software. Here the atomic functions were taken as double numerical bases with polarization functions (DNP).

The geometries were optimized by calculating the forces at each atomic site and moving the atoms along the path of steepest descent until the forces vanish. The threshold for the forces was set at 10^{-8} au/Bohr. This procedure does not guarantee that the system will find the global minimum structure as it can become stuck in local minima of the potential energy surface during optimization. Thus, one has to continue the optimization process from different starting configurations. For Mn_3 the initial configurations were chosen to be linear and triangular. For Mn_4 we used linear and planar rhombus as well as three dimensional (distorted tetrahedron) structures as starting geometries. For Mn_5, the starting geometries were confined to three different structures: a planar pentagon, a square pyramid and a triangular bipyramid.

Since the Mn atom has five unpaired spins, each of the geometry optimizations mentioned above has to be repeated for different spin multiplicities to determine the magnetic configuration of the ground state. For Mn_2 the possible spin multiplicities range from 1 to 11, while for Mn_3, Mn_4 and Mn_5 they range from 2 to 16, 1 to 21 and 2 to 26 respectively. These are very lengthy and complex calculations. To reduce the demand on computational time, we obtained the preferred spin multiplicity by first carrying out geometry and spin optimizations using the effective core potential (ECP) and LANL2DZ basis [21]. Once the preferred spin multiplicity at this level was obtained, we repeated all-electron calculations for this as well as neighbouring spin multiplicities to obtain the final results. We will show that the results obtained using ECP agree very well with the all-electron calculations. In the following we discuss our results.

3. Results

We divide this section into several parts. First, we discuss the accuracy of our approach by comparing the ionization potential and spin multiplicity of the Mn atom calculated using various levels of theory with experiments. We then discuss the geometry, electronic structure, ionization potential and magnetic properties of Mn clusters.

In table 1 we list the ionization potential and magnetic moment of the Mn atom calculated using different basis functions and various levels of correlation, and compare these results with experiment. All levels of theory give the correct magnetic moment of the atom, namely 5 μ_B. The ionization potentials calculated using the LSDA and B3LYP level of theory are essentially the same for the same basis function. It is hard to argue that the addition of the diffusion functions to the atomic basis leads to any significant improvement between theory and experiment for the atom. The GGA level of theory using the BPW91 procedure does not fare as well as the B3LYP form. We will show in the following that neither LSDA nor BPW91 correctly accounts for the properties of Mn_2, and that diffuse functions are essential to bind Mn_2 or larger clusters of Mn.

3.1. Mn_2 dimer

As outlined before, the atomic configuration of Mn is $3d^5\ 4s^2$. Because of the half filled 3d and filled 4s shell and the large promotion energy needed to change the occupation of the 3d and 4s levels (e.g. $3d^6\ 4s^1$), the Pauli principle prevents the two Mn atoms from coming close to each other. Consequently the binding of the atoms is weak and Mn_2 is believed to be a van der Waals molecule [3]. Calculations of the binding energy, bond length and

Table 1. Ionization potential (I.P.) and magnetic moment of Mn atom computed at various levels of theory and using different basis functions (basis 1: 14s 9p 5d 1f/9s 5p 3d 1f; basis 2: 15s 11p 6d 1f/10s 7p 4d 1f; LANL2DZ with effective core potential).

Level of theory	Basis set	Ionization potential (eV)	Magnetic moment (μ_B)
LSDA	LANL2DZ	7.88	5
	Basis 1	7.32	5
	Basis 2	7.52	5
BPW91	LANL2DZ	7.46	5
	Basis 1	6.89	5
	Basis 2	7.07	5
B3LYP	LANL2DZ	7.43	5
	Basis 1	7.36	5
	Basis 2	7.52	5
Expt		7.43	5

Table 2. A summary of binding energy (E_b), bond length (R_e) and magnetic moment, μ of Mn_2 calculated by various authors.

Authors	Method	E_b (eV)	R_e (Å)	μ (μ_B)
Nesbet [10]	RHF + Heisenberg exchange	0.79	2.88	0
Wolf and Schmidtke [11]	RHF		1.52	0
Shillady *et al* [14]	UHF	0.08	3.50	10
Harris and Jones [12]	LSDA	1.25	2.70	10
Salahub and Baykara [13]	LSDA	0.86	2.52	0
Fujima and Yamaguchi [15]	LSDA	$\sim$0.7	3.4	0
Expt [4]		0.1 ± 0.1	3.4	0
Matrix-isolated		0.56 ± 0.26	3.4	0

magnetic moment of Mn_2 date back to the early work of Nesbet [10] more than 30 years ago. In table 2 we summarize some of the earlier theoretical results. Nesbet calculated a $^1\Sigma_g^+$ ground state for Mn_2 at the restricted Hartree–Fock (RHF) level. He then calculated the energies of higher spin states by allowing spin-flip excitations to the antibonding levels. This resulted in $^9\Sigma_g^+$ being the lowest energy state. A Heisenberg-like treatment of the resulting atoms carrying 4 μ_B each led to the $^1\Sigma_g^+$ or antiferromagnetic ground state with a binding energy of 0.79 eV and bond length of 2.88 Å. Wolf and Schmidtke [11] also carried out a RHF calculation, but the bond length of their $^1\Sigma_g^+$ state was 1.52 Å, in sharp disagreement with the results of Nesbet. Shillady *et al* [14] carried out an unrestricted Hartree–Fock (UHF) calculation and found Mn_2 to be ferromagnetically coupled with a total moment of 10 μ_B, bond length of 3.50 Å and binding energy of 0.08 eV. We are not aware of any *ab initio* quantum chemical calculations that have gone beyond the Hartree–Fock theory.

Several calculations using the local spin density approximation in the density functional theory have been reported. Harris and Jones [12] found $^{11}\Pi_u^+$ and $^{11}\Sigma_u^+$ to be the lowest in energy with the same binding energy (1.25 eV) and similar bond lengths (2.66 Å and 2.7 Å respectively). They found the $^9\Sigma_g^+$ state to be unbound by 0.05 eV. Salahub and Baykara [13] have carried out broken-symmetry (two Mn atoms treated as inequivalent) calculations

at the LSDA level and found the ground state to be antiferromagnetic with a binding energy of 0.86 eV and bond length of 2.52 Å. Fujima and Yamaguchi [15] have carried out a spin-polarized discrete variational Xα (DV-Xα) method with numerical 1s–4s, 2p–4p and 3d atomic orbital bases. They also predict an antiferromagnetic ground state with a bond length of 3.4 Å and an estimated binding energy of $\sim$0.7 eV. We want to emphasize that the above basis is too limited to account for the weak interaction in the dimer. Until our recent work [22], no attempts beyond LSDA within the density functional theory had been available in the literature. We have also not seen attempts in the published literature to study systematically the energies for all possible spin multiplicities.

In order to understand the effect of basis sets and correlation, we have repeated the calculations for Mn_2 by using the local spin density approximation (LSDA) [18], BPW91 [19] and B3LYP [20] forms of the generalized gradient approximations (GGA) and three different basis sets. The results are summarized in tables 3 and 4. In table 3 we present the binding energy ($E_b = 2E(\mathrm{Mn}) - E(\mathrm{Mn_2})$) and bond lengths of Mn_2 corresponding to spin multiplicities of 1–11 obtained using the effective core potential (LANL2DZ basis) and the LSDA and GGA (B3LYP) level of correlation. Note that the singlet configuration is not bound at any level while states corresponding to spin multiplicities of 3, 7, 9 and 11 at the LSDA level of theory are all bound. At the GGA level, the configuration with a spin multiplicity of 11 is the only one bound. The equilibrium bond lengths steadily increase with increasing spin multiplicities. This is consistent with the physical picture that reduction of inter-atomic distance leads to stronger overlap of the atomic orbitals which, in turn, reduces the magnetic moment.

Table 3. Binding energies and equilibrium bond lengths of Mn_2 for spin multiplicities of 1, 3, 5, 7, 9 and 11 obtained using the LSDA and GGA (B3LYP) level of theories and LANL2DZ (effective core) basis.

	Bond length (Å)		Binding energy (eV)	
Spin multiplicity	LSDA	GGA	LSDA	GGA
1	1.66	1.65	Unbound	Unbound
3	1.66	1.65	0.525	Unbound
5	1.81	1.82	0.106	Unbound
7	1.96	2.26	0.624	Unbound
9	2.22	2.63	1.030	Unbound
11	2.50	3.50	1.378	0.11

In table 4 we present the binding energies, bond lengths, magnetic moments and adiabatic ionization potentials of the ground state of Mn_2 and Mn_2^+ using the all-electron extended basis as well as the effective core basis sets and different correlation potentials. Note that the B3LYP level of theory provides the best agreement for binding energy and the bond length of Mn_2 measured in a rare-gas matrix. But this theory predicts that Mn_2 has a magnetic moment of 10 μ_B. Unfortunately there are no experiments on free Mn_2 clusters to compare with our calculations. Baumann *et al* [4] have carried out electron spin resonance experiments on Mn_2 isolated in rare-gas matrices. Regardless of the matrix, as the temperature was raised above 4 K, an 11-line pattern was seen to grow. The absence of the 11-line spectra at 4 K and their rapid appearance with temperature led the authors to conclude that Mn_2 is diamagnetic in its lowest state and that spin unpairing is occurring at higher temperatures. Since Mn_2 itself is a very weakly bound molecule, one cannot rule out the possibility that the matrix may affect the magnetic properties of Mn_2, especially when

Table 4. Adiabatic ionization potential, binding energies, bond lengths and magnetic moments of Mn_2 and Mn_2^+ dimers using all-electron extended basis (basis 2) at various levels of theory (LSDA, BPW91 and B3LYP). Also given are results obtained using the LANL2DZ (ECP) basis with the B3LYP method.

Quantity	Levels of theory	Mn_2	Mn_2^+
Ionization potential (eV)	LSDA	6.65	
	BPW91	6.05	
	B3LYP	5.99	
	B3LYP (ECP)	6.29	
	Expt	6.9 ± 0.4	
Bond length (Å)	LSDA	1.62	2.43
	BPW91	2.60	2.95
	B3LYP	3.55	3.03
	B3LYP (ECP)	3.52	3.0
	Expt	3.4[a]	3.06[b]
Binding energy (eV)	LSDA	1.54	2.42
	BPW91	0.91	1.92
	B3LYP	0.06	1.59
	B3LYP (ECP)	0.11	1.69
	Expt	0.1 ± 0.1	0.85 ± 0.2
Magnetic moment (μ_B)	LSDA	2	9
	BPW91	10	11
	B3LYP	10	11
	B3LYP (ECP)	10	11
	Expt	0[a]	11[a]

[a] Estimated in rare-gas matrix.

[b] In MgO matrix.

The magnetic moment of the ground state of Mn_2 using the DMOL code is 10 μ_B both at LSDA and BPW91 levels of theory. The binding energy and bond length at LSDA level are 1.15 eV and 2.54 Å and at BPW91 level are 0.79 eV and 2.68 Å.

there are many low-lying states and that the ground state of Mn_2 in the beam may differ from that in the matrix.

To confirm whether the anti-ferromagnetic state could be lower in energy than the ferromagnetic state, we have repeated the calculations using the DMOL software at the LSDA level using the Vosko–Wilk–Nusair prescription [18] and at the GGA level using the Becke–Perdew–Wang (BPW91) scheme [19]. In the DMOL code [17] the orbitals are not symmetry adapted and the two Mn atoms are treated as distinct from each other. We have calculated the total energy of Mn_2 as a function of distance. At each distance the magnetic moment is computed by the Aufbau principle. The ground state was found to be ferromagnetic with a total moment of 10 μ_B at both LSDA and GGA levels of theory. The binding energy and bond length at LSDA level were 2.54 Å and 1.15 eV while at the GGA (BPW91) level they were 2.70 Å and 0.79 eV. While the results based on LSDA do not agree between the Gaussian and DMOL codes, those based on BPW91 do. We have also calculated the energetics of the anti-ferromagnetic state of Mn_2 in the DMOL code. The binding energy and bond length at the GGA level of theory (BPW91) were calculated to be 0.34 eV and 2.68 Å respectively. We should caution the reader that a binding energy of 0.79 eV is still too high to be characteristic of a van der Waals system. It is also important to realize that the density functional theory, even with GGA, may not be able

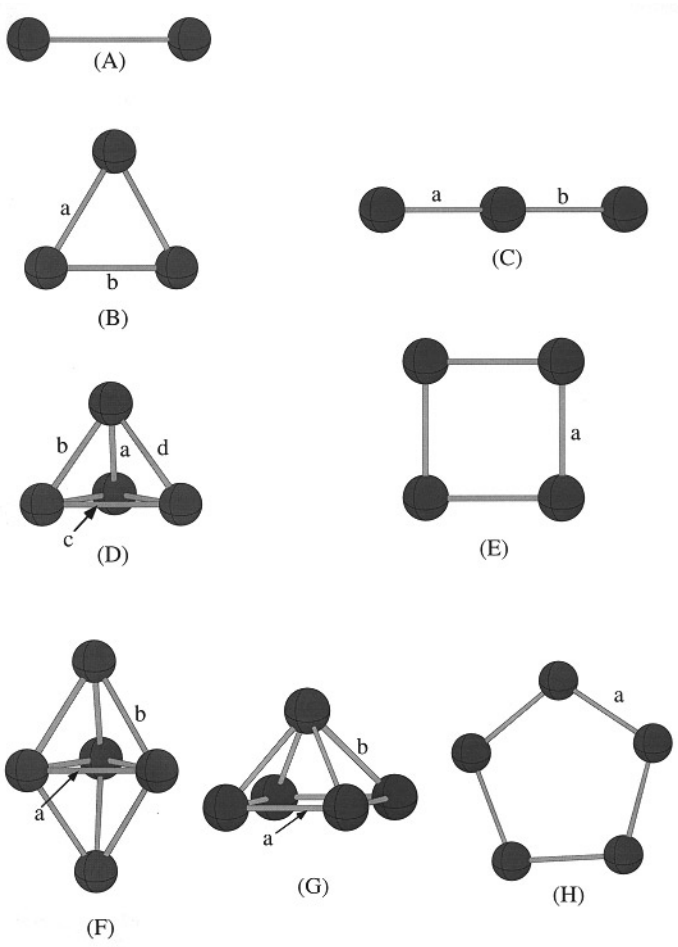

Figure 1. Optimized geometries of Mn_n ($n = 2$–5) clusters corresponding to the ground state (column 1) and higher energy isomers (columns 2 and 3). Bond lengths indicated in the figure are given in tables 5 and 6.

to treat the van der Waals interaction properly. The correlations, as measured in the van der Waals interactions, involves virtual atomic excitations which are not properly described in the free electron approximation. As pointed out in a recent calculation by Patton and Pederson [23], no mean field treatment is capable of reproducing the long range fluctuating dipole attraction in a closed shell system. Clearly further work is necessary in this regard. Patton and Pederson have systematically examined the binding energies and bond lengths of rare-gas dimers using LSDA and two forms of GGA. In comparision to the results of LSDA, GGA gives reasonable agreement with experiment. However, this agreement is still not complete.

It is, therefore, important to compare the theoretical results on Mn_2^+ with experiment using the same level of theories as discussed above. Note that Mn_2^+ is formed by removing an electron from the antibonding state of the 4s orbitals. This would cause Mn_2^+ to be better bound with regard to dissociated Mn and Mn^+ and the bond distance should decrease from that in Mn_2. In table 4 we see that the B3LYP level of theory correctly describes

this trend. Equally important is the effect of ionization on the magnetic moment of Mn_2^+. With an s electron removed from the anti-bonding state, the 4s states would contribute an additional 1 μ_B to the total magnetic moment. Since neutral Mn_2 has a magnetic moment of 10 μ_B, Mn_2^+ should have a moment of 11 μ_B. This is what the GGA level of theories in table 4 gives and agrees with experiment [24]. Although the magnetic experiment in Mn_2^+ was carried out in a rare-gas matrix, we do not expect the matrix to play as large a role as in Mn_2 since the binding energy of Mn_2^+ is significantly high. The calculated bond length at the B3LYP level of theory of Mn_2^+ also agrees with the experiment. Based upon this agreement, we believe that the B3LYP level of theory and the Gaussian 94 with the extended basis function will yield reliable results for larger Mn clusters. In the following we discuss the evolution of the equilibrium geometry, electronic structure, ionization potential and magnetic properties of Mn_3, Mn_4 and Mn_5 clusters.

3.2. Equilibrium geometries and energetics

In figure 1 we give the geometries corresponding to the ground state and next higher energy isomer of the Mn clusters. The binding energies ($E_b(\mathrm{Mn}_n) = nE(\mathrm{Mn}) - E(\mathrm{Mn}_n)$) of the clusters in their ground state along with their preferred magnetic moment calculated using the extended all-electron as well as the effective core (LANL2DZ) bases at the B3LYP level of theory are summarized in table 5. The energies of isomers measured with respect to the ground state energy as well as those of other low lying spin multiplets calculated using the LANL2DZ basis are given in table 6. We have identified two geometries of Mn_3. The equilibrium geometry is an equilateral triangle (see figure 1(B)) with a bond length of 2.88 Å and a binding energy of 0.74 eV. The Mn_3 forming a linear structure is a higher energy isomer that lies 0.55 eV above the ground state. Its inter-atomic distance is slightly reduced (2.78 Å) from that in the ground state structure (see table 6).

Table 5. Binding energies and magnetic moments of Mn_n ($n \leqslant 5$) clusters corresponding to their ground state calculated using all-electron extended basis (basis 2) and effective core (LANL2DZ) basis at the B3LYP level of theory. See figure 1 (first column) for corresponding geometries.

	Bond length (Å)		Binding energy/atom (eV)		Magnetic moment (μ_B)	
Cluster size, n	Basis 2	LANL2DZ	Basis 2	LANL2DZ	Basis 2	LANL2DZ
1					5	5
2	3.55	3.52	0.03	0.05	10	10
3	$a = b = 2.90$	$a = b = 2.88$	0.25	0.32	15	15
4	2.90, 2.85	2.90, 2.86	0.50	0.54	20	20
5	2.82, 2.91	2.84, 2.92	0.55	0.64	25	25

The ground state of Mn_4 is a nearly perfect tetrahedron with an inter-atomic distance that is almost identical with that in Mn_3. In a planar configuration, the local minimum of Mn_4 corresponds to a square geometry, but with an inter-atomic distance that is 0.2 Å shorter than the ground state structure. The binding energy/atom, although larger than that in Mn_3, remains relatively small compared to other transition metal clusters.

The geometries and electronic structure of Mn_5 are much more complex than those in smaller clusters. This is brought about by degeneracies not only between various structures but also different spin multiplicities. For example, the ground state of Mn_5 is a nearly perfect triangular bi-pyramid with a total moment of 25 μ_B. A square pyramid structure is nearly degenerate with the ground state geometry but has a different magnetic configuration

Table 6. Energies, ΔE of the some of the low lying spin states of Mn clusters measured with respect to the ground state structure. The effective core potential (LANL2DZ basis) was used for these calculations. Only those states that are bound with respect to the dissociated Mn atoms are given.

Cluster	Geometry	Spin multiplicity	Bond lengths (Å)	ΔE (eV)
Mn_3	Figure 1(B)	14	$a = 2.53$, $b = 2.78$	0.68
	Figure 1(C)	16	$a = b = 2.78$	0.55
		14	$a = b = 2.54$	0.72
Mn_4	Figure 1(D)	19	$a = c = 3.05$, $b = d = 2.65$	0.48
		17	$a = c = 2.70$, $b = d = 2.73$	1.39
	Figure 1(E)	19	$a = 2.63$	0.83
Mn_5	Figure 1(F)	24	$a = 2.72$, $b = 2.91$	0.04
		26	$a = 2.94$, $b = 2.84$	0.70
	Figure 1(G)	24	$a = 2.69$, $b = 2.76$	0.04
		22	$a = 2.83$, $b = 2.59$	1.00
		20	$a = 2.74$, $b = 2.56$	2.63
	Figure 1(H)	26	$a = 2.89$	1.35

and will be discussed later. The planar configuration of Mn_5 is a pentagon but is 1.35 eV higher in energy than the ground state. The inter-atomic distances in these structures range from 2.6 to 2.9 Å. However, the inter-atomic distances corresponding to the ground state geometries are nearly the same for Mn_3, Mn_4 and Mn_5.

3.3. Electronic structure

The energy levels of Mn_n clusters are shown in figure 2. As expected, in an atom, the highest molecular orbital has 4s character and is well separated from 3d orbitals (see figure 2(a)). The energy levels of Mn_2 are shown in figure 2(b). Here the 4s orbitals of two Mn atoms split into four molecular orbitals—one each for spin-up and spin-down bonding orbitals and the other two representing spin-up and spin-down antibonding orbitals. There is very little hybridization occurring between s and d orbitals as can be seen from a natural bond analysis (NBA) presented in table 7. Interestingly, the 3d orbitals combine to give rise to spin-up and spin-down bonding and antibonding orbitals where the minority levels lie much higher in energy compared to majority d (both bonding and antibonding) and s manifolds. As a result, all the d electrons occupy majority levels, giving ferromagnetic ordering in Mn_2. The energy levels for Mn_3 are shown in figure 2(c). It is to be noted here that the majority and minority levels of HOMO lie very close to each other. A population analysis shows that while the majority HOMO has completely s character (s = 97%), substantial hybridization between s and d occurs for minority levels (s = 62%, d = 32%). This gives rise to stronger bonding in Mn_3 compared to Mn_2 as is reflected in the increase in binding energy (see table 5). Further support of stronger hybridization is obtained from the decrease in the bond lengths in Mn_3 compared to Mn_2 (see table 5). However, there is almost no hybridization occurring in the energy levels lying below the HOMO. The energy levels of Mn_4 are shown in figure 2(d). The majority HOMO has s-type character with little hybridization (s = 96%, p = 4%) while the minority HOMO has almost the same mixing of s and d characters as in Mn_3 (s = 61%, d = 30%). This is reflected by the fact that while the binding energy and bond length change sharply in going from Mn_2 to Mn_3, they almost remain unchanged

in going from Mn_3 to Mn_4. A delicate situation occurs in Mn_5. The ground state of Mn_5 has degenerate structures (see table 6). For a better understanding, we compare the energy levels between the same structure (trigonal bipyramid) with spin states ($M = 26$, 24) in figure 2(e), (f). In contrast to smaller clusters discussed earlier, the energy levels of Mn_5 ($M = 26$) show strong mixing in s and d characters. Here, in addition to hybridization seen in the minority levels of HOMO, noticeable s–d hybridization occurs in the lower energy levels of the majority spin states as shown in figure 2(e). As a matter of fact, the energy levels of $M = 24$ shows that majority HOMO has substantial hybridization which is further supported by the natural bond analysis presented in table 7. As a result of s–d mixing in majority energy levels, the lower spin states are comparable in energy to that of the highest spin states.

Table 7. Natural bond analysis of the highest occupied molecular orbitals (HOMOs) of Mn_n clusters ($n \leqslant 5$) corresponding to the ground state structures.

Cluster	Figure	4s	3d	4p	5s	4d
Mn_2	1(A)	1.95	5.03	0.02		
Mn_3	1(B)	1.59	5.32	0.07	0.01	0.01
Mn_4	1(D)	1.56	5.30	0.12	0.01	0.01
Mn_5	1(F)	1.55	5.37	0.14	0.01	0.01
		1.53	5.23	0.08	0.02	0.01

3.4. Ionization potential

In figure 3 we plot the ionization potential of Mn_n clusters for $n \leqslant 5$ calculated using both the extended all-electron (basis 2) and the effective core (LANL2DZ) bases. The ionization potentials are quite high. Unfortunately there are no experimental measurements in this size range with which our theory can be compared. However, Koretsky and Knickelbein [9] have measured the ionization potentials of Mn_n clusters for the $7 \leqslant n \leqslant 64$ size range. The ionization potentials range from 4.35 eV to 5.44 eV. They have set a lower limit of 6.4 eV for the ionization potentials of Mn clusters. Since our calculated energies reproduce experimental values to within 0.5 eV, the results in figure 3 may be argued to be consistent with the experimental upper limit.

3.5. Magnetic moments

We now discuss what we believe to be the most interesting results in Mn clusters, namely magnetism. As pointed out earlier for Mn_2, the ground state was found to be ferromagnetic with a total moment of 10 μ_B. Mn_3, Mn_4 and Mn_5 carry 15 μ_B, 20 μ_B and 25 μ_B magnetic moments in their ground state configurations. These large magnetic moments arise as each Mn atom carries a moment of 5 μ_B and all the moments are ferromagnetically aligned.

In table 3 and the earlier part of this paper we have discussed at length the energetics of Mn_2 for different spin multiplicities. In table 6 we give the energetics and geometrical parameters of Mn_3, Mn_4 and Mn_5 corresponding to low-lying spin multiplicities and structures for which the clusters are bound against dissociation into free atoms. For Mn_3, an isosceles triangular structure with a magnetic moment of 13 μ_B is bound, but it lies 0.68 eV above the ground state. In the linear configuration, the structure with a magnetic moment of 15 μ_B is more stable than that with 13 μ_B, but both of these configurations lie

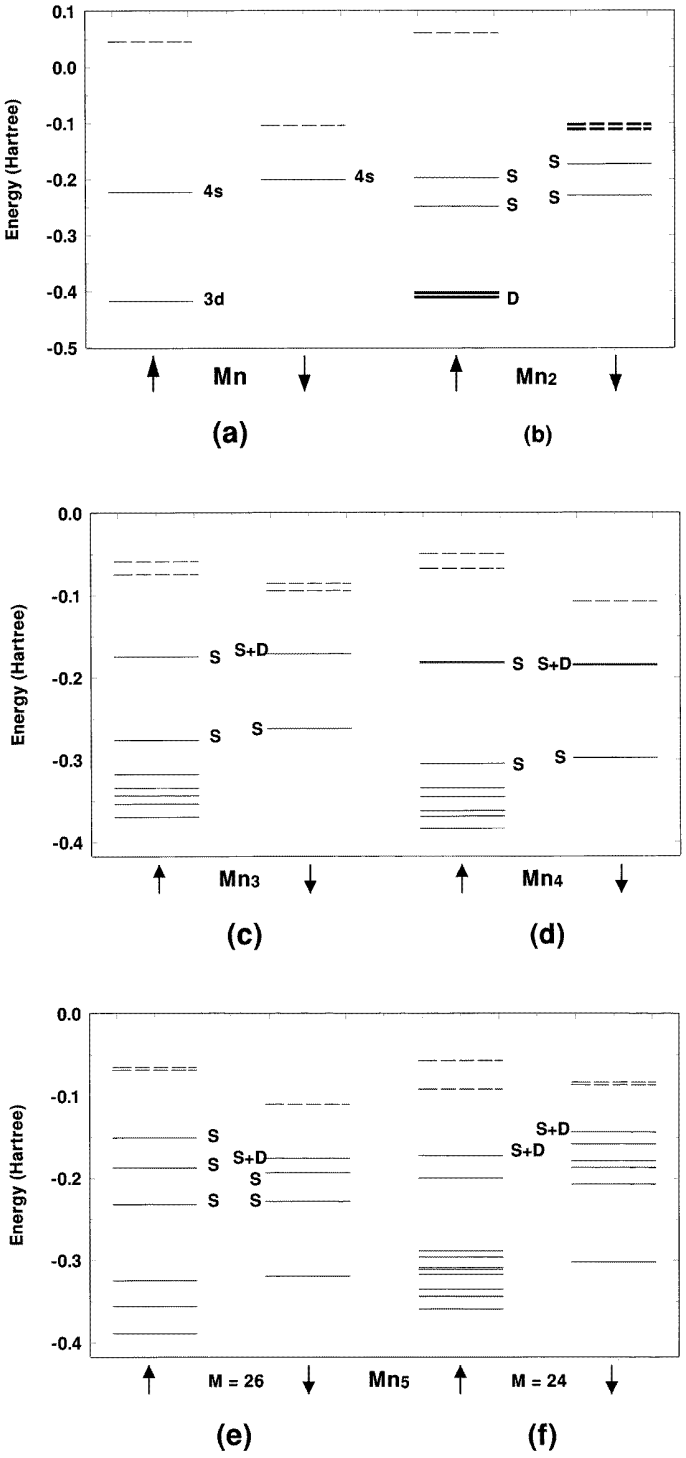

Figure 2. One-electron energy levels for spin up (↑) and spin down (↓) orbitals of (a) Mn, (b) Mn_2, (c) Mn_3, (d) Mn_4 and (e), (f) Mn_5. The symbol next to the lines indicates the nature of the molecular orbitals. See the text for details.

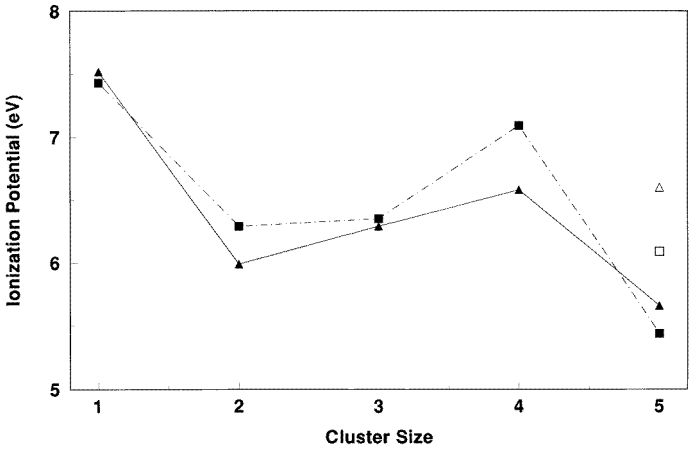

Figure 3. Plot of ionization potential (I.P.) as a function of cluster size. The solid line corresponds to all-electron calculation while the dotted line corresponds to calculation using LANL2DZ basis sets. Open square and open triangle correspond to I.P. of Mn_5 isomer with figure 1(G) geometry obtained using all-electron extended and LANL2DZ basis sets.

0.55 eV and 0.72 eV above the ground state. Thus, we can conclude that Mn_3 does not have a nearly degenerate isomer.

The same is true for Mn_4. There are two Jahn–Teller distorted tetrahedral structures with magnetic moments of 18 μ_B and 16 μ_B that lie 0.48 eV and 1.39 eV above the ground state. In the planar configuration, Mn_4 assumes a square geometry with a magnetic moment of 18 μ_B. Again, it is 0.83 eV above the ground state structure that carries 20 μ_B magnetic moment.

The situation with Mn_5 is more complex than those discussed above. Not only does Mn_5 exist in other isomeric forms, but also it carries different magnetic moments in the respective equilibrium structures that are nearly degenerate with the ground state. For example, a slightly distorted triangular bipyramidal structure with a magnetic moment of 23 μ_B is only 0.04 eV above the 25 μ_B ground state structure. Similarly, a square pyramidal structure with a moment of 23 μ_B is nearly degenerate with the ground state structure. This indicates that as cluster size increases, there will be an increasing number of isomers with different magnetic moments that may be nearly degenerate. Thus, understanding of the magnetic transition from ferromagnetic to anti-ferromagnetic configurations with increasing cluster size may not be trivial.

Unfortunately, as mentioned earlier, there are no experiments where magnetic moments of Mn clusters in the gas phase have been measured. However, experiments on Mn_4 and Mn_5 isolated in matrices are available. Ludwig *et al* [25] have studied Mn_4 in solid silicon. They have observed a 21-line hyperfine pattern that not only establishes the four atoms to be equivalent, but also the total moment of Mn_4 to be 20 μ_B. This result is consistent with our result in table 5. Baumann *et al* [4] have carried out electron spin resonance studies of Mn_5 isolated in a rare-gas matrix. They have measured a magnetic moment of 25 μ_B and have suggested that the structure could be a pentagon, triangular bipyramid or square pyramid. Our results in table 5 and the degeneracies in structures and spin multiplicities are certainly consistent with their conclusion.

In spite of this agreement in the magnetic moment, one must wonder whether the matrix does play a role. This can only be achieved by measuring the magnetic moments of Mn

clusters in the beam. This certainly will be an important experiment as we predict that moment/atom in small Mn cluster will retain its free atomic value. No element in the periodic table, to our knowledge, shares this distinction.

It is worth noting that the magnetism of Mn in the form of supported clusters and monolayers [26, 27] have been studied theoretically. Here, the ferromagnetic and anti-ferromagnetic solutions are nearly degenerate. More interestingly, the moment/atom is nearly 5 μ_B. In the Heusler alloys X_2MnY (X = Cu, Y = Sn), although none of the elements are ferromagnetic, the alloy is ferromagnetic with a moment of 5 μ_B localized at the Mn site. Thus, while bulk Mn is anti-ferromagnetic, evidence suggests that Mn in reduced size and dimension could be ferromagnetic with very large moments/atom.

4. Conclusions

In summary, we have carried out self-consistent calculations of the geometries, total energies, electronic structure and magnetic properties of small Mn clusters using a number of theoretical techniques and numerical procedures. Our most important conclusions are: (1) The binding of Mn_2 is very weak and is of the van der Waals type. As the number of atoms in the cluster increases, there is increasing hybridization between 3d and 4s states. This leads to improvements in the binding energies, but it remains weak compared to other transition-metal clusters in the same size range. (2) The equilibrium geometries are fairly compact and symmetric with very little Jahn–Teller distortion. For Mn_5 there are isomers whose energies lie very close to the energy of the ground state. This is not the case in smaller clusters. (3) The inter-atomic distance is large for the Mn_2 dimer and decreases sharply in Mn_3. The average inter-atomic distances in Mn_4 and Mn_5 do not change very much from that in Mn_3 and compare favourably with the bulk values that range from 2.25 Å to 2.95 Å depending on the various allotropic forms of the Mn crystal. (4) The magnetic moments/atom in the clusters retain their value in the free atom, namely 5 μ_B/atom. The clusters are ferromagnetic in that all the moments are aligned in the parallel direction. The Mn_2 dimer has been found to have a moment of 10 μ_B while the experiment in the rare-gas matrix yields an antiferromagnetic state. It is difficult to resolve this discrepancy as there are no experiments in the gas phase. This is particularly problematic [28] for Mn_2 because it is very weakly bound. Its properties can be easily affected by the matrix and/or deficiencies in the theoretical approach as discussed earlier. For Mn_2^+ and larger Mn clusters where binding is significant, these problems are less severe. It is encouraging that the calculated magnetic moments of Mn_3, Mn_4 and Mn_5 which are respectively 15 μ_B, 20 μ_B and 25 μ_B agree with the matrix isolated experimental results. The calculated ionization potentials are also consistent with the upper limit set by experiments. (5) Both the extended nature of the basis sets and an accurate description of correlation are important to achieve a quantitative understanding of the properties of Mn clusters.

It is hoped that these results will stimulate measurements of the magnetic moments of Mn clusters in the beam. It will be interesting to see how large an Mn cluster needs to be before the magnitude of the moment/atom is less than 5 μ_B, and the coupling changes from ferromagnetic to anti-ferromagnetic. In particular, it will be interesting to see if the dependence of reactivity on cluster size is mirrored in the magnetic moment measurements.

Acknowledgments

This work is supported in part by a grant from the Department of Energy (DEFG05-87E61316). The authors are grateful to Dr A K Rajagopal for many stimulating discussions.

References

[1] Moore C E 1952 *Natl. Bur. Stand. (US), Circ.* **467** 27
[2] Arrott A 1966 *Magnetism* vol 2B, ed G T Rado and A Suhl (New York: Academic) p 295
[3] Morse M D 1986 *Chem. Rev.* **86** 1049
[4] Baumann C A, VanZee R J, Bhat S and Weltner W Jr 1983 *J. Chem. Phys.* **78** 190
[5] Nayak S K, Khanna S N, Rao B K and Jena P 1997 *J. Phys. Chem.* A **101** 1072
[6] Reuse F, Khanna S N, de Coulon V and Buttet J 1989 *Phys. Rev.* B **39** 12 911
[7] Rademann K, Kaiser B, Evan U and Hensel F 1987 *Phys. Rev. Lett.* **59** 2319
Brechignac C, Broyer M, Cahuzac Ph, Delacretaz G, Labastie P, Wolf J P and Wöste L 1988 *Phys. Rev. Lett.* **60** 275
[8] Parks E K, Nieman G C and Riley S J 1996 *J. Chem. Phys.* **104** 3531
[9] Koretsky G M and Knickelbein M B 1997 *J. Chem. Phys.* **106** 9810
[10] Nesbet R K 1964 *Phys. Rev.* **135** A460
[11] Wolf A and Schmidtke H-H 1980 *Int. J. Quantum Chem.* **18** 1187
[12] Harris J and Jones R O 1979 *J. Chem. Phys.* **70** 830
[13] Salahub D R and Baykara N A 1985 *Surf. Sci.* **156** 605
Salahub D R 1987 *Ab Initio Methods in Quantum Chemistry II* ed K P Lawley (New York: John Wiley)
[14] Shillady D D, Jena P, Rao B K and Press M R 1988 *Int. J. Quantum Chem.* **22** 231
[15] Fujima N and Yamaguchi T 1995 *J. Phys. Sols Japan* **64** 1251
[16] Frisch M J *et al* 1995 *Gaussian 94* revision B.1 (Pittsburgh, PA: Gaussian)
[17] Biosym *DMOL Code* (San Deigo, CA: Biosym)
[18] Vosko S H, Wilk L and Nusair M 1980 *Can. J. Phys.* **58** 1200
[19] Becke A D 1988 *Phys. Rev.* A **38** 3098
Perdew J P and Wang Y 1992 *Phys. Rev.* B **45** 13 244
[20] Lee C L, Yang W and Parr R G 1988 *Phys. Rev.* B **37** 785
Becke A D 1993 *J. Chem. Phys.* **98** 5648
[21] Hay P J and Wadt W R 1985 *J. Chem. Phys.* **82** 270
Wadt W R and Hay P J 1985 *J. Chem. Phys.* **82** 299
[22] Nayak S K and Jena P 1998 *Chem. Phys. Lett.* **289** 473
[23] Patton D C and Pederson M R 1997 *Phys. Rev.* A **56** R2495
[24] Van Zee R J and Weltner W Jr 1988 *J. Chem. Phys.* **89** 4444
[25] Ludwig G W, Woodbury H H and Carlson R O 1959 *J. Phys. Chem. Solids* **8** 490
[26] Stepanyuk V S, Hergert W, Wildberger K, Nayak S K and Jena P 1997 *Surf. Sci. Letts.* **384** L892
[27] Blügel S, Drittler B, Zeller R and Dederichs P H 1989 *Appl. Phys.* A **49** 547
[28] After this manuscript was prepared we received a preprint by Pederson, Reuse and Khanna who have calculated the equilibrium geometries and magnetic moments of small Mn clusters using density functional theory, Gaussian basis sets and the generalized gradient approximation due to Becke–Perdew–Wang. They too find the Mn clusters to be ferromagnetic with a magnetic moment of nearly 5 μ_B per atom. In particular, they find Mn_2 to be ferromagnetic with 10 μ_B magnetic moment. Their computed bond length of 2.61 Å and binding energy of 0.99 eV are close to our BPW91 result but differ from our B3LYP calculations as well as from experiments. The authors have not computed the properties of Mn_2^+.